

**Modeling streamflow using multiple precipitation products in a topographically complex catchment**

Author

Usman, Muhammad, Ndehedehe, Christopher, Manzanas, Rodrigo, Adeyeri, Oluwafemi

Published

2022

Journal Title

Modeling earth systems and environment

Version

Accepted Manuscript (AM)

DOI

[10.1007/s40808-021-01198-1](https://doi.org/10.1007/s40808-021-01198-1)

Rights statement

© 2022 Springer Nature Switzerland AG. This is an electronic version of an article published in Modeling Earth Systems and Environment, 2022, 8 (2), pp. 1875-1885. Modeling Earth Systems and Environment is available online at: <http://link.springer.com/> with the open URL of your article.

Downloaded from

<http://hdl.handle.net/10072/418074>

Griffith Research Online

<https://research-repository.griffith.edu.au>

1 **Modeling streamflow using multiple precipitation products in a**  
2 **topographically complex catchment**

3

4 **Muhammad Usman<sup>1\*</sup>, Christopher E. Ndehedehe<sup>2</sup>, Burhan Ahmad<sup>1</sup>, Rodrigo Manzanas<sup>3</sup>,**  
5 **and Oluwafemi E. Adeyeri<sup>4,5</sup>**

6

7 <sup>1</sup>Pakistan Meteorological Department, Pitras Bukhari Road, H-8/2, Islamabad, Pakistan

8 <sup>2</sup>Australian Rivers Institute and Griffith School of Environment & Science, Griffith University, Nathan,  
9 Queensland 4111, Australia

10 <sup>3</sup>Meteorology Group, Dpto. de Matemática Aplicada y Ciencias de la Computación, Universidad  
11 de Cantabria, Santander, 39005, Spain

12 <sup>4</sup>Department of Meteorology and Climate Science, Federal University of Technology, Akure,  
13 Nigeria

14 <sup>5</sup>Institute for Meteorology and Climate Research, Karlsruhe Institute of Technology, Campus  
15 Alpine, Garmisch-Partenkirchen, Germany

16 **Abstract**

17 Precipitation is of primary importance in hydrological modeling and predicting streamflow.  
18 However, lack of gauged stations for long term precipitation data particularly in the data scarce  
19 Chitral River Basin (CRB) of Pakistan and other parts of developing world is a hindrance to  
20 understanding surface water hydrology. Therefore, this study aims to assess different sources of  
21 precipitation data for streamflow prediction in the CRB. A modified version of conceptual and  
22 semi-distributed hydrological model Hydrologiska Byråns Vattenbalansavdelning (HBV) known  
23 as HBV-light is used in this study to model streamflow by forcing it with precipitation inputs of  
24 different Precipitation Products (PPs). These PPs include, APHRODITE (V1101, V1801R1),  
25 CHIRPS V2.0, CPC-Global, ERA5, GPCC V.2018 (V2), GPCP-1DD V1.2, PERSIANN,  
26 PERSIANN CCS, PERSIANN CDR, and TRMM (3B42V7). The model was calibrated and  
27 validated for two periods (1995–2005 and 2007–2013, respectively), and showed good  
28 performance during both periods. Prior to assessing the performance of these PPs to simulate  
29 observed streamflow, they were assessed against gauged precipitation. Results of this study  
30 suggest that APHRODITE-based precipitation performed better than other precipitation products  
31 in the simulation of precipitation characteristics in the study region. Multiple efficiency evaluation  
32 metrics including KGE, NSE, and PBIAS were employed to assess streamflow prediction  
33 capability of different products. Results indicated that APHRODITE outperformed all other

34 precipitation products ( $KGE = 0.89$ ) in terms of simulating observed streamflow in the CRB. The  
35 CPC Global precipitation product ( $KGE = 0.71$ ) was found to be the least suitable product for  
36 hydrological modeling in the CRB. This study provides useful guidance for the selection and  
37 application of gridded precipitation products for long term continuous streamflow prediction in  
38 the Chitral River Basin.

39 **Keywords:** Streamflow prediction, Chitral River Basin., PCA, HBV-light, Gridded precipitation,  
40 Reanalysis, APHRODITE

41

## 42 **Introduction**

43 Understanding of hydrological implications of climatic variability is crucial for sustainable  
44 freshwater resources management (Ndehedehe et al. 2020), and hydrological modeling is widely  
45 used to improve understanding of hydrological processes (Beven 2011; Pakoksung and Takagi  
46 2016; Belayneh et al. 2020; Kabood et al. 2020). Management of freshwater resources is also an  
47 integral part of food security and functioning of various ecosystems (e.g. aquatic biodiversity)  
48 (Agutu et al. 2019; Schroth et al. 2016; Cenacchi 2014; Tockner et al. 2010). One of the most  
49 important driving forces of a hydrological model and a component of the hydrological cycle is  
50 precipitation (Beck et al. 2017; Masih et al. 2010; Price et al. 2014). Characteristically,  
51 precipitation is highly variable, and its estimation is difficult, especially in regions with complex  
52 topography (Stephens et al. 2010; Herold et al. 2016; Prein and Gobiet 2017). It is also crucial for  
53 simulation of streamflow (Sun et al. 2018; Pena Arancibia et al. 2013) and better understanding of  
54 hydrometeorological processes (Hu et al. 2017; Ma et al. 2015).

55 Globally, there is a decline in gauged observations for precipitation due to lack of investment in  
56 gauge measurements (e.g., Ndehedehe 2019a). Even for regions with observational networks, their  
57 density falls below the World Meteorological Organization guidelines (Vorosmarty et al. 2001).  
58 Chitral River Basin (CRB) is in a geopolitical zone of Pakistan in the famous Hindukush-  
59 Karakoram-Himalayan (HKH) region and has shared transboundary water resources with  
60 Afghanistan. Both countries are emerging economies and depend on this shared natural resource  
61 (Biermann and Dingwerth 2004). These riparian countries not only face climate-induced  
62 adversities and variations in the hydrological cycle within their own boundaries but also across the  
63 borders, and this situation could lead to altercation and unrest on both sides (Wolf 2009). This calls

64 for a revision of the existing water related policies (which are inclined more towards national or  
65 sub-national frontiers) and transfer to new policies with a focus on transboundary menaces  
66 (Hashmi et al. 2019).

67 Recently, there have been some recommendations and guidelines in other regions of the world to  
68 address issues related to transboundary water resources and conflicts. And problems associated  
69 with transboundary water resources has resulted in water diplomacy and institutional framework  
70 that could be used to nurture the cooperation among different stakeholders (Akhmadiyeva and  
71 Abdullaev 2019; Atef et al. 2019; Ndehedehe et al. 2020). Water diplomacy is considered as one  
72 of the best choices in terms of relevant tools when it comes to the shared management of  
73 transnational water resources, engagement of political and institutional dialogues, and policies to  
74 keep up fruitful discussions related to different aspects of water sharing (e.g. legal) and to improve  
75 the functionality of transboundary water cooperation (Honkonen and Lipponen 2018, Grech-  
76 Madin et al. 2018; Schmeier and Shubber 2018).

77 To devise a policy that could account for the resolutions and better management of water resources,  
78 a good start would be the understanding of surface water hydrology and its relation key  
79 components of the water cycle (like precipitation). However, a key problem that arises is the lack  
80 of sufficient gauge data for hydrological applications, which creates a gap in knowledge, especially  
81 in understanding the complexity of natural processes and important drivers of surface water  
82 hydrology. As with other emerging economies, available ground precipitation data in Pakistan and  
83 specifically in the CRB are limited, which is a hurdle in detailed assessments of hydrological  
84 processes (Cogley 2009; Hewitt 2011; Adnan et al. 2017). Satellite and reanalysis based gridded  
85 precipitation products are among alternate sources of precipitation data. These observations have  
86 a high potential for freshwater resource management in the data-scarce regions and are becoming  
87 increasingly popular and widely used in surface water hydrology related studies (e.g. Li et al. 2018;  
88 Agutu et al. 2017; Ndehedehe et al. 2020). Recent studies in the African regions with limited  
89 gauging stations, for example, have successfully utilized different alternative precipitation  
90 products to understand the regional hydrology and the dynamics of freshwater resources  
91 (Skaskevych et al. 2019; Ndehedehe et al. 2018, 2019b).

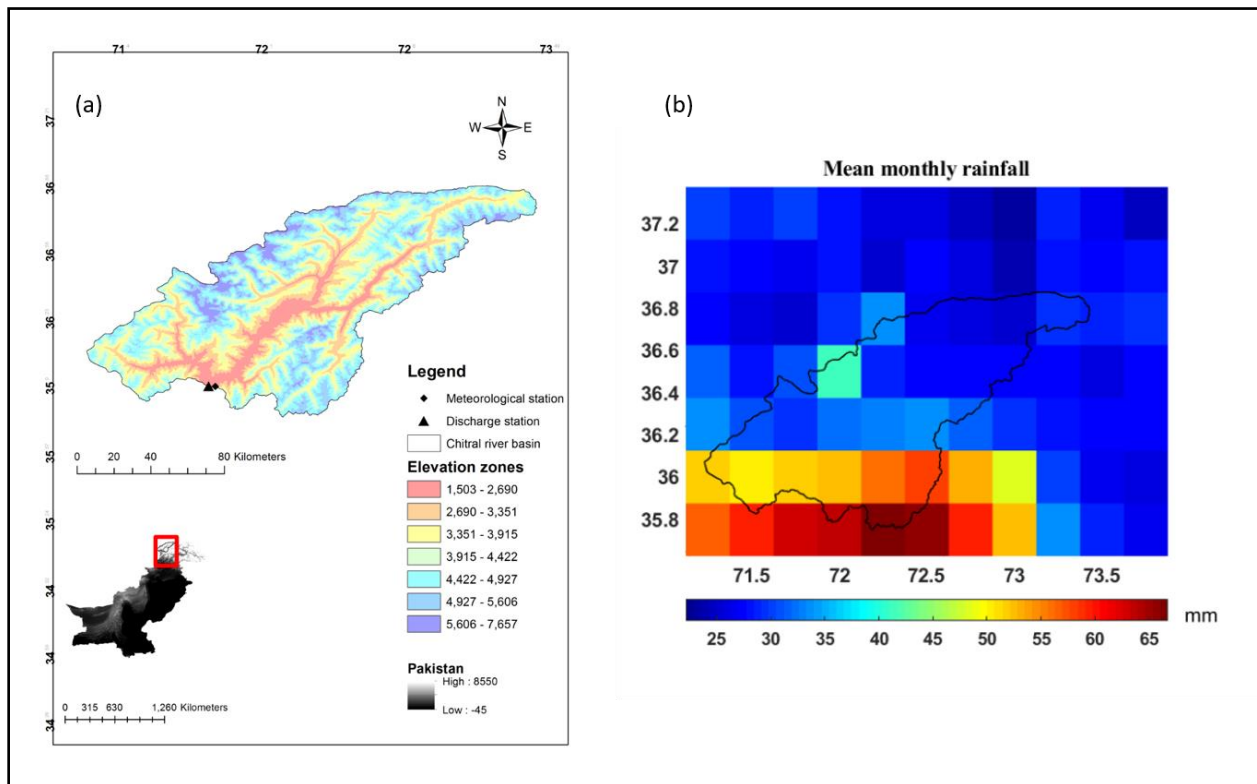
92 To our knowledge, the performance evaluation of different precipitation products for streamflow  
93 prediction, in the CRB has not been reported. This study therefore aims to evaluate efficiency of

94 different Precipitation Products (PPs) for streamflow prediction in the data-scarce region of CRB  
95 using hydrological modeling. The specific objectives of this study are to: (1) evaluate the  
96 performance of ten different precipitation products with respect to gauge precipitation in the CRB  
97 and (2) investigate the performance of these precipitation products for streamflow prediction.

## 98 **Materials and Methods**

### 99 **Study area**

100 The Chitral River is one of the most important rivers of the Hindukush ranges, in the Hindukush-  
101 Karakoram-Himalayan region. It covers an area of 11,396 km<sup>2</sup> and elevation in the CRB ranges  
102 from about a 1000 m to more than 7500 m above mean sea level (Fig. 1). It is one of the most  
103 topographically complex catchments and is in the humid region of Pakistan. Maximum  
104 precipitation is received in winter and spring (Hayat et al. 2019). CRB is bordered by Afghanistan  
105 in the west and river water is crucial for two nations to support their domestic activities and  
106 requirements, and for nurturing the socio-economic development of the region.



107  
108 **Fig. 1** (a) Physical characteristics and location map of the study area (b) mean monthly rainfall  
109 over the catchment

110 **Hydrological model and input data**

111 The Hydrological Bryans Vattenbalansavdelning HBV is a simple bucket type model (Bergström  
112 1976; Lindström et al. 1997) used for streamflow simulation. In this study, a modified version of  
113 the model i.e. the HBV-light (Seibert and Vis 2012) is used, which has been extensively used  
114 worldwide (Vis et al. 2015; Hakala et al. 2018; Usman et al. in press). It is termed as a semi-  
115 distributed model, as spatial discretization of catchment (into different elevation and vegetation  
116 zones) is possible. Precipitation, air temperature, and estimated potential evapotranspiration data  
117 is used as input data in the HBV-light. Detailed description of the model can be found in (Siebert  
118 and Vis 2012; Bergström 1976; Lindström et al. 1997, Burhan et al. 2020). The Digital Elevation  
119 Model (DEM) was obtained from the Shuttle Radar Topographic Mission (SRTM) with a spatial  
120 resolution of approximately 90 m. Potential evapotranspiration was calculated using the method  
121 proposed by (Irmak et al. 2003).

122 **Precipitation Products (PPs)**

123 Ten different precipitation products are evaluated in this study to predict streamflow, details of the  
124 products including spatial and temporal resolutions, available periods, and respective references  
125 are summarized in Table 1.

126 Table 1. Characteristics of precipitation datasets used in this study.

Datasets (short name)	Spatial resolution	Temporal resolution	Period (used in this study)	Reference
APHRODITE V1101, V1801R1	0.25°	daily	1995-2013	(Yatagai et al. 2012),
CHIRPS V2.0	0.25°	daily	1995-2013	(Funk et al. 2015)
CPC-Global	0.5°	daily	1995-2013	(Xie et al. 2010)
ERA5	0.25°	daily	1995-2013	Copernicus Climate Change Service (C3S) (2017)
GPCC V.2018 (V2)	1°	daily	1995-2013	(Schamm et al. 2014)
GPCP-1DD V1.2	1°	daily	October 1996- 2013	(Huffman et al. 2001)
CHRS PERSIANN	0.25°	daily	March 2000- 2013	(Sorooshian et al. 2000)
CHRS CCS	0.25°	daily	2003-2013	(Hong et al. 2004)
CHRS CDR	0.25°	daily	2003-2013	(Ashouri et al. 2015)
TRMM 3B42 V7	0.25°	daily	1998-2013	(Huffman et al. 2007)

127

128 **Model calibration and validation**

129 The HBV-light was calibrated with observed precipitation data as an input for a period of 1995-  
130 2005 with a spin up period of a year 1994, and validated for a period of 2007-2013 with a spin up  
131 period of a year 2006. Then the model was recalibrated for each satellite precipitation product.  
132 Model efficiency was evaluated using three different evaluation criteria i.e. Kling-Gupta  
133 Efficiency (KGE) (Gupta et al. 2009), Percent Bias (PBIAS), and the Lindström measure (Lm)  
134 (Lindström et al. 1997). Lm incorporates combined effects of two widely used metrics (Hakala et  
135 al. 2018) i.e. the Nash-Sutcliffe efficiency (NSE); (Nash and Sutcliffe 1970) and volume error.  
136 The Lindström measure is calculated as “NSE minus 0.1 multiplied by the relative volume error”  
137 (Hakala et al. 2018). KGE and Lm has a perfect value of 1, and PBIAS has a perfect value of 0,  
138 which shows the highest possible match between observed and modeled streamflow. Genetic  
139 algorithm and Powell optimization (GAP; Seibert 2000) method is an automatic calibration  
140 method, in which the selection of optimum parameters is done first, and then a fine tuning is done  
141 to further enhance the objective function. The HBV-light was calibrated using GAP and Powell  
142 optimization.

143 **Statistical decomposition of precipitation**

144 Single meteorological station is used in this study as this is the only station in the catchment with  
145 a relatively long-term data (i.e., greater than fifteen years). Some other important questions prior  
146 to our analysis are; what is the magnitude of spatial precipitation in that location where the gauge  
147 is located in comparison to other areas within the basin? How spatially variable is precipitation in  
148 the study area? So, the spatial and temporal patterns of precipitation in the whole catchment were  
149 analyzed to examine if this meteorological station captures the plenitude and magnitude of  
150 precipitation observed in the catchment. To this end, a statistical decomposition of precipitation  
151 grids into spatial and temporal patterns using the principal component analysis [PCA, (Jolliffe  
152 2002)] was undertaken. The scree plot analysis was used to identify two significant modes of  
153 precipitation variability in the basin. No fixed criterion is established to define the number of  
154 substantial principal components (PCs) that are best reserved in a particular situation, however,  
155 the selection of truncation can differ from existing selection rules to more subjective picks (e.g.,  
156 scree plot analysis) depending on the data and the purpose of the statistical rotation (see, e.g.,  
157 Ndehedehe et al. 2020b; Wilks 2011; Martinez and Martinez 2005). In the statistical rotation of  
158 precipitation using the PCA method, a deseasonalized matrix of precipitation grids (i.e., after

159 removal of the mean) masked over the Chitral catchment would be given as equation 1  
 160  $C_{precipitaion} = [z(\mathbf{u}_p, t)]$  where  $\mathbf{u}_p$  is spatial locations;  $p = 1, 2, \dots, nz$ , which depicts the number  
 161 of spatial locations for  $C_{precipitaion}$ , and  $t$  is the monthly time step from 2002 to 2018 i.e., temporal  
 162 evolutions). As an illustrative example, the  $0.25^\circ$  monthly precipitation grids over the CRB for the  
 163 period between 2002 and 2018,  $C_{j \times h}$  will have the size,  $j = 183$  and  $h = 96$  where  $j$  and  $h$  are the  
 164 monthly time steps (2002 to 2018) and observations (precipitation grids over the Chitral  
 165 catchment), respectively (Ndehedehe et al. 2020b). The statistical decomposition of precipitation  
 166 grids into spatio-temporal patterns using this method is given as (Ndehedehe et al. 2019c),

$$167 \quad C_{precipitaion}(t) = \sum_{p=1}^n m_p \mathbf{u}_p \quad 1$$

168 Where  $m_p(t)$  are the temporal variations also known as expansion coefficients, which have been  
 169 normalized using their standard deviation to make them unit free and  $\mathbf{u}_p$  are the corresponding  
 170 spatial maps (empirical orthogonal functions-EOF loadings). Usually the principal components  
 171 (PCs) of these loadings are used to adjust (scale) them to their original units (millimeter), they  
 172 provide the weights of the original variables employed in the PCs. This approach provides the  
 173 knowledge of the distribution of precipitation in time and space over the CRB.

174 **Methodology to evaluate the efficiency of PPs in simulating observed precipitation and**  
 175 **streamflow**

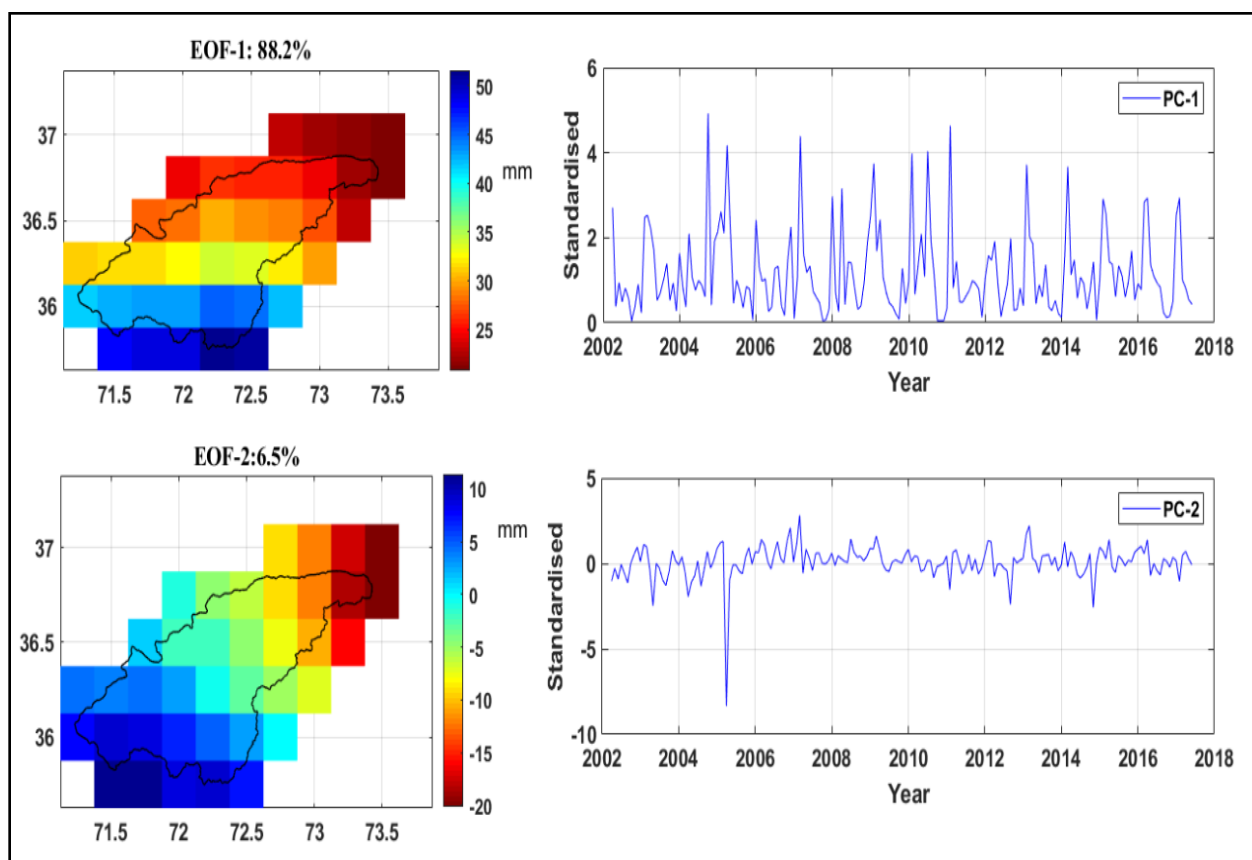
176 Ten different PPs were evaluated against the gauge-based precipitation and then were used as  
 177 forcing data to drive the HBV-light to simulate the observed streamflow. For comparison of  
 178 precipitation of PPs and observed precipitation, all precipitation products were evaluated using  
 179 correlation co-efficient  $R^2$ . As the major objective of this study was to analyze the performance of  
 180 different precipitation products in predicting streamflow, other statistical criteria including KGE,  
 181 NSE, and PBIAS were also used to evaluate the efficiency of the products in simulating observed  
 182 streamflow. We evaluated performance of ten different PPs in their native resolution without any  
 183 rescaling algorithms to avoid associated uncertainties (Hu et al. 2018). These precipitation  
 184 products are often used to derive precipitation at a local scale without any added adjustments  
 185 (Zandler et al. 2019), therefore, this approach was selected.

186 **Results**

187 **Spatio-temporal variability of precipitation**



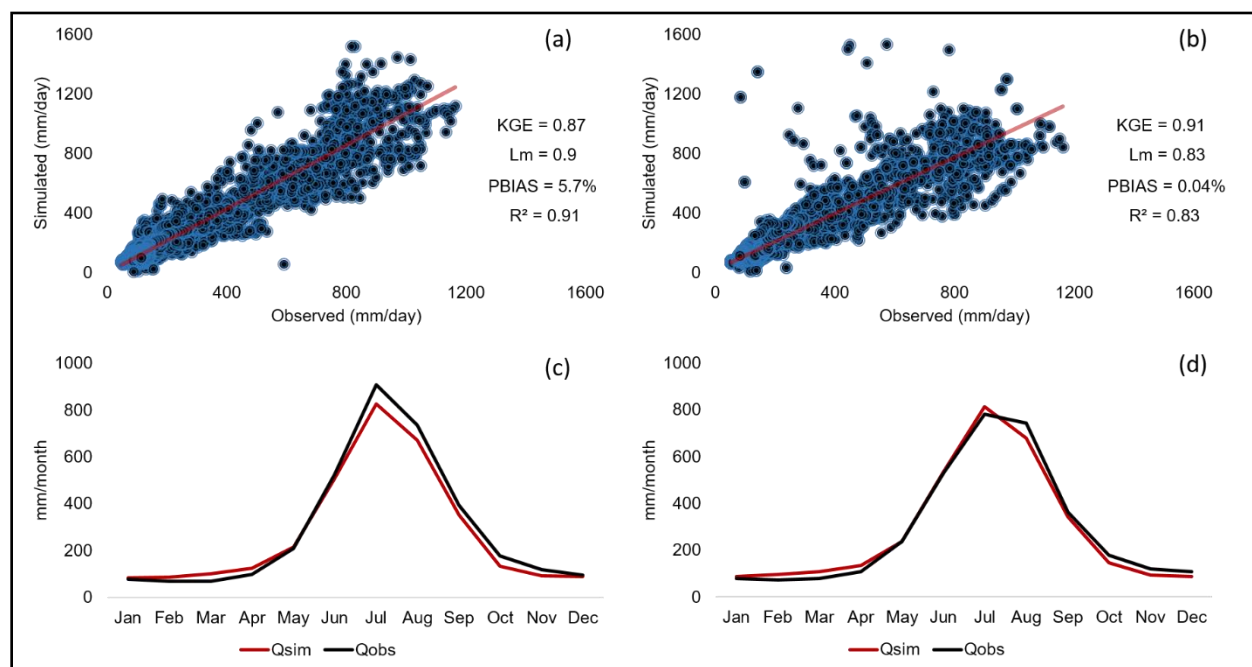
188 A preliminary analysis of satellite precipitation over the catchment show that the first orthogonal  
 189 mode of precipitation accounts for more than 88 % of observed total variability. The strongest  
 190 loadings or spatial patterns are localized over the south where the gauged station is located as  
 191 opposed to the dry northern section of the basin (EOF-1, Fig. 2). While this emphasizes the  
 192 importance of assessing the hydrological processes of the south in terms of rainfall-runoff  
 193 modeling, it justifies the use of this meteorological station in this study. This assumption holds  
 194 given the observed magnitude of precipitation in the sub-grids of the vicinity where the station  
 195 data used in the validation of precipitation products is located (Fig 1). The temporal patterns (PC-  
 196 1, Fig. 2) associated with this leading mode of precipitation show considerable inter-annual  
 197 fluctuations. The spatio-temporal variability of precipitation in the second mode (PC-2/EOF-2,  
 198 Fig. 2) accounts for only 6.5 % and indicates short-term seasonal signals not relevant to the current  
 199 analysis.



200  
 201 **Fig. 2** Spatial and temporal analysis of precipitation over the CRB using TRMM-based  
 202 precipitation (2002-2018). The EOFs (left) are the spatial patterns of rainfall associated with the  
 203 temporal patterns on the right (principal components).

## 204 Calibration and validation of the HBV-light

205 For the calibration and validation of the model, values of different metrics that were achieved show  
206 a good performance of the model in capturing observed streamflow. For the calibration period, Lm  
207 value of 0.9 was achieved, and for the validation period, Lm value of 0.83 was achieved. Similarly,  
208 for the calibration period, a KGE value of 0.87 was achieved, and for the validation period a KGE  
209 value of 0.91 was achieved. PBIAS between the observed and modeled streamflow was 5.7 %  
210 during calibration period and 0.04 % during validation period. These results show that the HBV-  
211 light have performed remarkably well in the CRB. Comparison of observed and simulated  
212 streamflow in the CRB at daily and monthly time scales during calibration and validation periods  
213 is shown in (Fig. 3), which highlights the model's performance. Hydrological modeling approach  
214 was then used for assessing efficiency of different PPs.

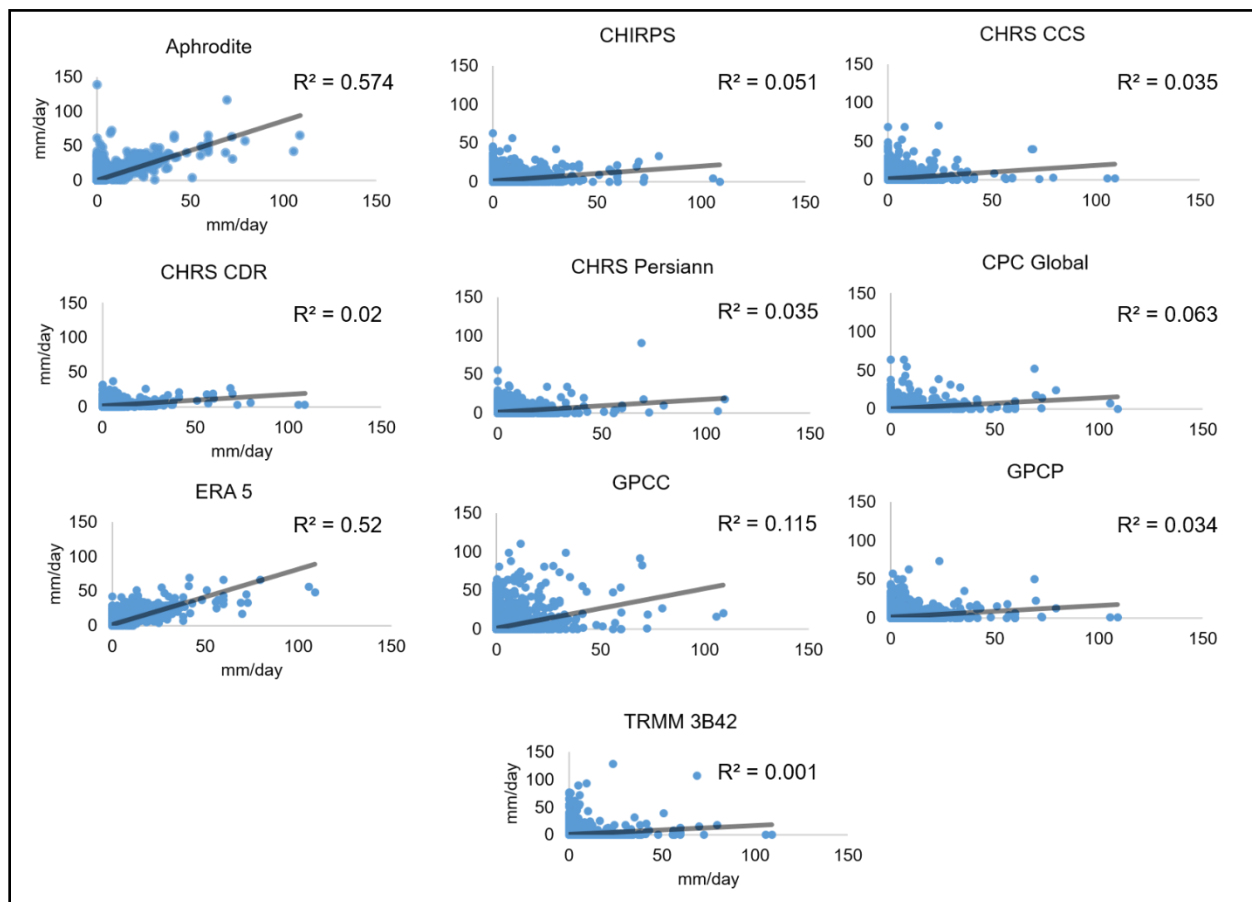


215  
216 **Fig. 3** Observed and simulated streamflow during calibration and validation periods. (a) Daily  
217 calibration 1995-2005 (b) daily validation 2007-2013 (d) monthly calibration 1995-2005 (d)  
218 monthly validation 2007-2013

## 219 Efficiency evaluation of different PPs in simulating observed precipitation

220 The classic statistical measure, i.e., the correlation coefficient ( $R^2$ ) between gauge-based and  
221 products-based daily precipitation is depicted in (Fig. 4). Range of  $R^2$  for daily precipitation  
222 between observed and satellite-based products is from 0.001 to 0.574. Best representative of the

223 observed precipitation in terms of  $R^2$  is the APHRODITE precipitation product and the least  
 224 correlation with the observed precipitation is shown by TRMM 3B42 (Fig. 4).



225  
 226 **Fig. 4** Performance of different precipitation products in capturing observed precipitation.

227 **Efficiency evaluation of the predicted streamflow using different PPs**

228 The calibrated and validated model was forced with precipitation data of different PPs to simulate  
 229 streamflow. KGE, NSE, and PBIAS have been selected to assess their performance. The  
 230 performance indices include KGE ranging from 0.71 to 0.89, NSE from 0.78 to 0.87, and PBIAS  
 231 ranging from -24 % to 17 % (Table 2). Results of the predicted streamflow indicated that  
 232 APHRODITE outperformed all other products in simulating streamflow KGE = 0.89, NSE = 0.87,  
 233 and PBIAS = 1 %. Some other products showed relatively better performance but not as optimum  
 234 as APHRODITE.

235

236

237

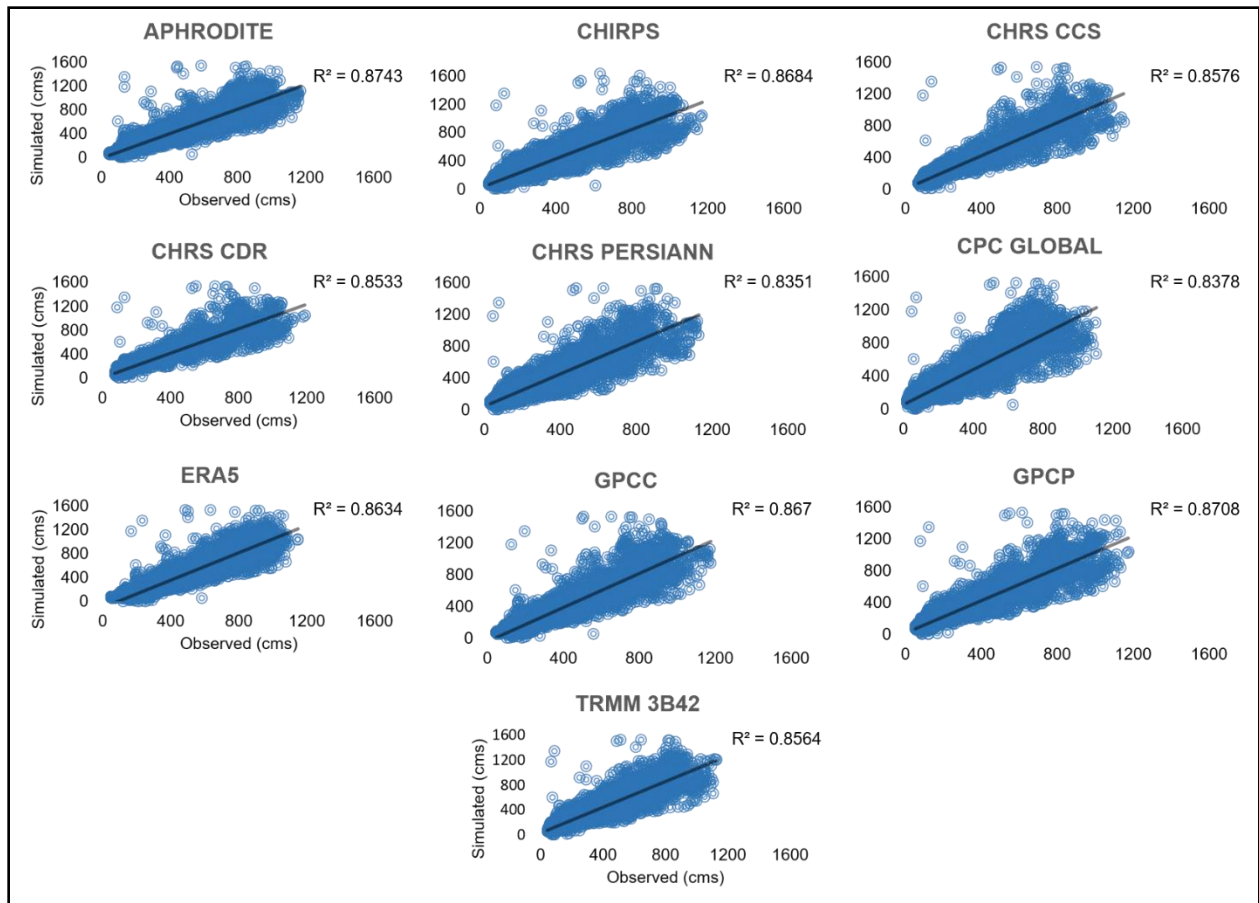
238 Table 2. Evaluation metrics for assessing streamflow prediction.

Precipitation product	KGE	PBIAS (%)	NSE
APHRODITE	0.89	1	0.87
CHIRPS	0.85	-9	0.86
CHRS CCS	0.86	-4	0.85
CHRS CDR	0.87	-4	0.85
CHRS PERSIANN	0.79	-16	0.81
CPC	0.71	-24	0.78
ERA5	0.73	17	0.82
GPCC	0.84	7	0.86
GPCP	0.86	-8	0.86
TRMM	0.81	-14	0.84

239

240 Correlation between streamflow predicted by different precipitation products and observed  
241 precipitation is shown in (Fig. 5). Apparently, Aphrodite performed better overall compared to  
242 other products in simulating observed streamflow.

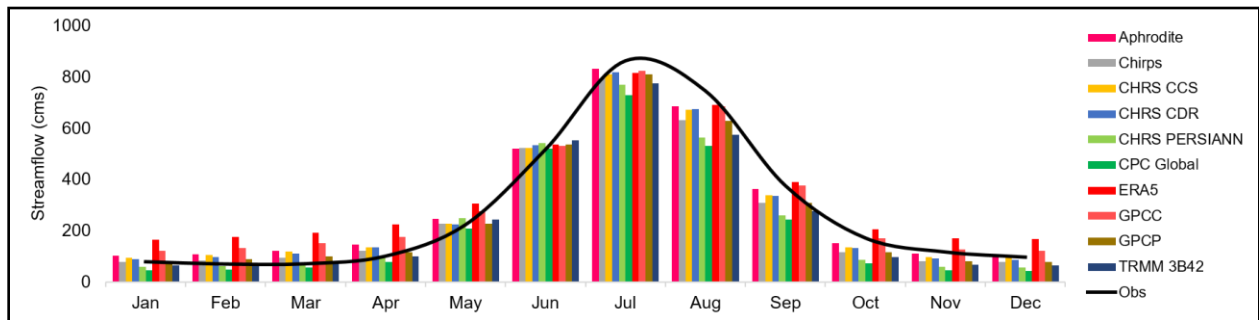
243 During dry period of the year, we note that streamflow is overestimated by ERA 5 followed by  
244 GPCC, APHRODITE, and CHRS CCS while it is underestimated by CPC Global followed by  
245 CHRS PERSIANN, TRMM 3B42, CHIRPS, GPCP, and CHRS CDR (Fig. 6) (mentioned in the  
246 order of maximum to minimum). However, in the wet period of the year, all the precipitation  
247 products have underestimated streamflow except the ERA 5 and GPCC, which overestimated the  
248 streamflow. Overall, the performance of APHRODITE is relatively better than other products  
249 throughout the year even with overestimation and underestimation in different periods.



250

251 **Fig. 5** Predicted streamflow by different precipitation products with respect to daily observed  
 252 streamflow.

253



254

255 **Fig. 6** Observed and simulated (using different precipitation products) monthly streamflow.

256 KGE is considered as the most important metrics for streamflow simulation (Brocca et al. 2020)  
 257 and has been given a significant weight in overall assessment of streamflow prediction ability of  
 258 different precipitation products. APHRODITE with maximum KGE, NSE, and minimum Percent

259 bias (negligible overestimation) was found to be the most appropriate precipitation product that  
260 could be used for hydrological modeling in the CRB.

261 Different products seem appropriate for the purpose of streamflow prediction in the CRB.  
262 However, their suitability is season dependent, that is, if their performance is better in one half of  
263 the year it is worse in other half. For instance, CHRS CDR has a KGE = 0.87, NSE = 0.85, and  
264 PBIAS of only -4 %, and it predicted the streamflow very efficiently during the dry period of the  
265 year with an average monthly streamflow of 100 m<sup>3</sup>/s compared to the observed average  
266 streamflow of 101 m<sup>3</sup>/s. However, when it comes to streamflow prediction in wet period of the  
267 year, it appears to underestimate streamflow significantly (453 m<sup>3</sup>/s as compared to 470 m<sup>3</sup>/s which  
268 is observed streamflow).

269 The other product that performed well was CHRS CCS, indicating a KGE = 0.86, NSE = 0.85, and  
270 PBIAS of only -4 %. It predicted streamflow more efficiently in the dry period of the year with an  
271 average monthly streamflow of 107 m<sup>3</sup>/s compared to the observed average streamflow of 101  
272 m<sup>3</sup>/s. However, when it comes to streamflow prediction during wet period, it underestimates  
273 streamflow (451 m<sup>3</sup>/s as compared to 470 m<sup>3</sup>/s, which is observed streamflow).

274 Moreover, we found that GPCP has also performs well in terms of statistical criteria evaluation  
275 with KGE, NSE, and PBIAS of 0.86, 0.86, and -8 % respectively. However, it underestimates the  
276 streamflow in dry period and even more in the wet period of the year. Average predicted  
277 streamflow in dry period by GPCP is 90 m<sup>3</sup>/s compared to 101 m<sup>3</sup>/s observed streamflow and  
278 average predicted streamflow in wet period (437 m<sup>3</sup>/s) compared to 470 m<sup>3</sup>/s (observed  
279 streamflow).

280 APHRODITE was the only precipitation product that outperformed other products in terms of the  
281 statistical evaluation metrics used in this study (KGE, NSE, R<sup>2</sup>, PBIAS), and streamflow prediction  
282 both in dry and wet period of the year. Average predicted streamflow in dry period by the  
283 APHRODITE-based precipitation is 116 m<sup>3</sup>/s compared to 101 m<sup>3</sup>/s (observed streamflow) and  
284 average predicted streamflow in wet period is 465 m<sup>3</sup>/s unlike observed streamflow which is 470  
285 m<sup>3</sup>/s.

## 286 **Discussion**

287 Modeling streamflow using a hydrological model is one of the widely used method to assess the  
288 suitability of different precipitation products for streamflow prediction. In this study, gauged based  
289 streamflow data were used for performance assessment of ten different Precipitation Products  
290 (PPs). As shown in this study, the hydrological model HBV-light performed considerably well  
291 both during calibration and validation periods. The results of this calibrated model indicate a high  
292 correlation between observed streamflow (monitored at the gauge) and the streamflow simulated  
293 by the model. This correlation ( $KGE = 0.87$  and  $0.91$  during calibration and validation  
294 respectively) is an indication of minimal errors of model structure, parameters and atmospheric  
295 forcings (Hakala et al. 2010). After the model setup, the next step was to assess the performance  
296 of ten different PPs, each of which have their own characteristics. The performance evaluation was  
297 carried out in two phases. In the first phase, efficiency of the precipitation products in replicating  
298 gauged-based precipitation was assessed, and in the second phase, the performance of these  
299 products in predicting observed streamflow was evaluated. Prior to conducting this two-phase  
300 analysis, an important preliminary aspect of this study was to assess whether the gauged  
301 precipitation data (consisting of one meteorological station) was good enough to capture the  
302 patterns of spatial and temporal variability within the whole basin or not. To this end, the Principal  
303 Component Analysis (PCA) technique was employed to decompose satellite-based rainfall into  
304 leading modes of variability. We found that more than 88 % of the changes in precipitation within  
305 the basin occurred around the point where the gauge is located. After this, the two-phase analysis  
306 of performance evaluation was then undertaken.

307 PPs used in this study among others have been evaluated in different regions of the world for  
308 understanding of hydrometeorological processes. Results of several such studies are location-  
309 specific, which implies that a dataset that has performed better in one region, might depict good or  
310 poor performance in another region. For instance, Guo et al. (2015) found out that TRMM  
311 performed better while CHRS PERSIANN could not achieve good correlation coefficients in the  
312 Central Asia region. On the contrary, in our study (which is in South Asia) CHRS PERSIANN  
313 performed better than TRMM. On the other hand there are instances, where a particular SPP was  
314 found to be perform well in different parts of the world, e.g. results of this study indicated that  
315 APHRODITE has better performance in terms of simulating observed precipitation over a complex  
316 terrain catchment in Pakistan. Tan et al. (2015) also reported that APHRODITE performed best  
317 over Malaysia, which suggests that a precipitation product that performs better over Malaysia also

318 has a good performance over Pakistan (even though different regions in both countries have  
319 different climatic characteristics). Results from our study are also consistent with those of Thom  
320 et al. (2017) and Ji et al. (2020) who argued that the APHRODITE datasets indicated good  
321 performance as input data to a hydrological model, performing well over Asia.

322 Furthermore, results in this study are align with the findings of Ménégoz et al. (2013), who  
323 suggested that the APHRODITE dataset was one of the most accurate precipitation products for  
324 Asia. Lauri et al. (2014) and Chen et al. (2017) also found out that APHRODITE was the best  
325 performing precipitation product for runoff simulations. Moreover, Li et al. (2018) showed that  
326 APHRODITE was a better choice for hydrological studies in Western Himalayas, which is also  
327 one of the most topographically complex regions in Asia. Vu et al. (2011) also reported that  
328 APHRODITE performed better for streamflow simulation in a study conducted over a river basin  
329 in Vietnam. The use of APHRODITE in hydro-ecological applications and modeling of water  
330 resources thus offer opportunities to fill gaps in gauged measurements in this data-deficient region.

### 331 **Conclusions**

332 The importance of consistent and long-term streamflow records to understand surface hydrology  
333 is well recognized. This is particularly true for different regions of developing world where long  
334 term data is scarce because of limited gauging stations. This study investigated the potential of ten  
335 different Precipitation Products (PPs), namely APHRODITE (V1101, V1801R1), CHIRPS V2.0,  
336 CPC-Global, ERA5, GPCC V.2018 (V2), GPCP-1DD V1.2, PERSIANN, PERSIANN CCS,  
337 PERSIANN CDR, and TRMM (3B42V7) using a hydrological modeling to predict streamflow in  
338 one of the most topographically complex catchments of the high mountain Asia i.e. the Chitral  
339 River Basin (CRB). A key aspect of assessing PPs performance to predict streamflow is to improve  
340 the modeling of streamflow using a hydrological model. In this study we used the hydrological  
341 model HBV-light to simulate streamflow in the CRB. Key findings of this study are summarized  
342 as follows.

- 343 • The Hydrological model's performance was good in modeling observed streamflow  
344 evidenced in the calibration (1995-2005) and validation (2007-2013) periods.
- 345 • APHRODITE was the most efficient precipitation product that captured gauged  
346 precipitation in comparison to other products in simulating observed precipitation.



- 347 • Different PPs including, CHRS CDR, CHRS CCS, and GPCP showed a good potential to  
348 be used for streamflow prediction. However, their good performance was season  
349 dependent, i.e., the performance was good in the dry period of the year but poor during the  
350 wet half of the year.
- 351 • The APHRODITE-based precipitation showed a better performance for streamflow  
352 prediction throughout the year unlike other PPs in this topographically complex terrain and  
353 catchment of the Chitral River Basin.

354 These results are promising and could be helpful for understanding of the hydrological processes  
355 in the region as well as sustainable management of freshwater resources.

### 356 **Funding**

357 We received no financial support for the research, authorship, and/or publication of this article.

### 358 **Conflict of Interest:**

359 Authors declare no conflict of interest.

### 360 **Data availability:**

361 Data is available from authors upon reasonable request.

### 362 **Acknowledgements:**

363 We are grateful to the Pakistan Meteorological Department and Surface Water Hydrology Group  
364 of Water and Power Development Authority of Pakistan for providing hydro-meteorological data  
365 for this study.

### 366 **References**

367 Adnan M, Nabi G, Poomee MS, Ashraf A (2017) Snowmelt runoff prediction under changing  
368 climate in the Himalayan cryosphere: A case of Gilgit River Basin. *Geosci Front* 8:941-949.  
369 <https://doi.org/10.1016/j.gsf.2016.08.008>

370  
371 Vörösmarty C, Askew A, Grabs W, Barry RG, Birkett C, Kitaev L (2001) Global water data: A  
372 newly endangered species. *Eos Trans AGU* 82:54-58. <https://doi.org/10.1029/01EO00031>

373  
374 Agutu NO, Awange JL, Ndehedehe C, Kirimi F, Kuhn M (2019) GRACE-derived groundwater  
375 changes over Greater Horn of Africa: Temporal variability and the potential for irrigated  
376 agriculture. *Sci Total Environ* 693:133467. <https://doi.org/10.1016/j.scitotenv.2019.07.273>

377

378 Agutu NO, Awange JL, Zerihun A, Ndehedehe CE, Kuhn M, Fukuda Y (2017) Assessing multi-  
379 satellite remote sensing, reanalysis, and land surface models' products in characterizing  
380 agricultural drought in East Africa. *Remote Sens Environ* 194:287-302.  
381 <https://doi.org/10.1016/j.rse.2017.03.041>  
382

383 Akhmadiyeva Z, Abdullaev I (2019) Water management paradigm shifts in the Caspian Sea  
384 region: Review and outlook. *J Hydrol* 568:997-1006.  
385 <https://doi.org/10.1016/j.jhydrol.2018.11.009>  
386

387 Atef SS, Sadeqinazhad F, Farjaad F, Amatya DM (2019) Water conflict management and  
388 cooperation between Afghanistan and Pakistan. *J Hydrol* 570:875-892.  
389 <https://doi.org/10.1016/j.jhydrol.2018.12.075>  
390

391 Ashouri HK, Hsu L, Sorooshian S et al (2015) PERSIANN-CDR: Daily precipitation climate  
392 data record from multisatellite observations for hydrological and climate studies. *Bull Amer*  
393 *Meteor Soc* 96:69-83. <https://doi.org/10.1175/BAMS-D-13-00068.1>

394 Beck HE, Vergopolan N, Pan M et al (2017) Global-scale evaluation of 22 precipitation datasets  
395 using gauge observations and hydrological modeling. *Hydrol Earth Syst Sci* 21:6201-6217.  
396 <https://doi.org/10.5194/hess-21-6201-2017>

397 Belayneh A, Sintayehu G, Gedam K, Muluken T (2020) Evaluation of satellite precipitation  
398 products using HEC-HMS model. *Model Earth Syst Environ* 6:2015-2032.  
399 <https://doi.org/10.1007/s40808-020-00792-z>

400 Beven KJ (2011) *Rainfall-runoff modelling: the primer*. John Wiley & Sons.

401 Bergström S (1976) Development and application of a conceptual runoff model for Scandinavian  
402 catchments. SMHI Norrköping, Report RH07. Retrieved from  
403 <http://urn.kb.se/resolve?urn=urn:nbn:se:smhi:diva-5738>

404 Biermann F, Dingwerth K (2004) Global environmental change and the nation state. *Glob Environ*  
405 *Politics* 4:1-22. <https://doi.org/10.1162/152638004773730185>  
406

407 Burhan A, Usman M, Bukhari SAA, Sajjad H 2020. Contribution of Glacier, Snow and Rain  
408 Components in Flow Regime Projected with HBV Under AR5 Based Climate Change Scenarios  
409 Over Chitral River Basin (Hindukush Ranges, Pakistan). *Int J Clim Res* 4:24-36.  
410 <http://www.conscientiabeam.com/journal/112/abstract/5965>  
411

412 Cenacchi N (2014) Drought risk reduction in agriculture: a review of adaptive strategies in East  
413 Africa and the indo-Gangetic plain of South Asia (Vol. 1372). *Intl Food Policy Res Inst.*  
414 Discussion Paper 1372 Retrieved from.  
415 <http://ebrary.ifpri.org/cdm/ref/collection/p15738coll2/id/128277> 23 September, 2017.  
416

417 Cogley JG (2009) Geodetic and direct mass-balance measurements: comparison and joint  
418 analysis. *Ann Glaciol* 50: 96-100. <https://doi.org/10.3189/172756409787769744>  
419

420 Copernicus Climate Change Service (C3S) (2017) ERA5: Fifth generation of ECMWF  
421 atmospheric reanalyses of the global climate. Copernicus Climate Change Service Climate Data  
422 Store (CDS), date of access July 2020.  
423 <https://cds.climate.copernicus.eu/cdsapp#!/home>  
424

425 Chen CJ, Senarath SU, Dima-West IM, Marcella MP (2017) Evaluation and restructuring of  
426 gridded precipitation data over the Greater Mekong Subregion. *Int J Climatol* 37:180-196.  
427 <https://doi.org/10.1002/joc.4696>

428 Funk C, Peterson P, Landsfeld M et al (2015) The climate hazards infrared precipitation with  
429 stations—a new environmental record for monitoring extremes. *Sci Data* 2:1-21.  
430 <https://doi.org/10.1038/sdata.2015.66>

431 Grech-Madin C, Döring S, Kim K, Swain A (2018) Negotiating water across levels: A peace and  
432 conflict “Toolbox” for water diplomacy. *J Hydrol* 559:100-109.  
433 <https://doi.org/10.1016/j.jhydrol.2018.02.008>  
434

435 Gupta HV, Kling H, Yilmaz KK, Martinez GF (2009) Decomposition of the mean squared error  
436 and NSE performance criteria: Implications for improving hydrological modelling. *J Hydrol* 377:  
437 80-91. <https://doi.org/10.1016/j.jhydrol.2009.08.003>  
438

439 Ji X, Li Y, Luo X et al (2020) Evaluation of bias correction methods for APHRODITE data to  
440 improve hydrologic simulation in a large Himalayan basin. *Atm Res* 242:104964.  
441 <https://doi.org/10.1016/j.atmosres.2020.104964>

442 Hashmi MZUR, Masood A, Mushtaq H, Bukhari SAA, Ahmad B, Tahir AA (2020) Exploring  
443 climate change impacts during first half of the 21st century on flow regime of the transboundary  
444 Kabul River in the Hindukush region. *J Water Clim Change* 11:1521-1538.  
445 <https://doi.org/10.2166/wcc.2019.094>

446 Herold N, Alexander LV, Donat MG, Contractor S, Becker A (2016) How much does it rain over  
447 land? *Geophys Res Lett* 43:341-348. <https://doi.org/10.1002/2015GL066615>

448 Hewitt K (2011) Glacier change, concentration, and elevation effects in the Karakoram Himalaya,  
449 Upper Indus Basin. *Mt Res Dev* 31:188-200. <https://doi.org/10.1659/MRD-JOURNAL-D-11-00020.1>  
450

451

452 Hong Y, Hsu KL, Sorooshian S, Gao X (2004) Precipitation estimation from remotely sensed  
453 imagery using an artificial neural network cloud classification system. *J Appl Meteorol* 43:1834-  
454 1853.  
455 <https://doi.org/10.1175/JAM2173.1>  
456

457 Honkonen T, Lipponen A (2018) Finland’s cooperation in managing transboundary waters and the  
458 UNECE Principles for Effective Joint Bodies: Value for water diplomacy? *J Hydrol* 567:320-331.  
459 <https://doi.org/10.1016/j.jhydrol.2018.09.062>  
460

461 Hu M, Sayama T, Duan W, Takara K, He B, Luo P (2017) Assessment of hydrological extremes  
462 in the Kamo River Basin, Japan. *Hydrolog Sci J* 62:1255-1265.  
463 <https://doi.org/10.1080/02626667.2017.1319063>  
464

465 Hu Z, Zhou Q, Chen X et al (2018) Evaluation of three global gridded precipitation data sets in  
466 central Asia based on rain gauge observations. *Int J Climatol* 38:3475-3493.  
467 <https://doi.org/10.1002/joc.5510>

468 Huffman GJ, Adler RF, Morrissey MM et al (2001) Global precipitation at one-degree daily  
469 resolution from multisatellite observations. *J Hydrometeorol* 2:36-50.  
470 [https://doi.org/10.1175/1525-7541\(2001\)002%3C0036:GPAODD%3E2.0.CO;2](https://doi.org/10.1175/1525-7541(2001)002%3C0036:GPAODD%3E2.0.CO;2)

471 Huffman GJ, Bolvin DT, Nelkin EJ et al (2007) The TRMM multisatellite precipitation analysis  
472 (TMPA): Quasi-global, multiyear, combined-sensor precipitation estimates at fine scales. *J*  
473 *Hydrometeorol* 8:38-55. <https://doi.org/10.1175/JHM560.1>

474 Jolliffe IT (2002) *Principal component analysis*. Springer Series in Statistics, second edition.  
475 Springer, New York.

476 Kabood SHT, Hosseini SA, Kabood AHT (2020) Investigating the effects of climate change on  
477 stream flows of Urmia Lake basin in Iran. *Model Earth Syst Environ* 6:329-339.  
478 <https://doi.org/10.1007/s40808-019-00681-0>

479 Lauri H, Räsänen TA, Kummu M (2014) Using reanalysis and remotely sensed temperature and  
480 precipitation data for hydrological modeling in monsoon climate: Mekong River case study. *J*  
481 *Hydrometeorol* 15:1532-1545. <https://doi.org/10.1175/JHM-D-13-084.1>

482 Li H, Haugen JE, Xu CY (2018) Precipitation pattern in the Western Himalayas revealed by four  
483 datasets. *Hydrol. Earth Syst Sci* 22:5097-5110. <https://doi.org/10.5194/hess-22-5097-2018>

484 Lindström G, Johansson B, Persson M, Gardelin M, Bergström S (1997) Development and test  
485 of the distributed HBV-96 hydrological model. *J Hydrol* 201:272-288.  
486 [https://doi.org/10.1016/S0022-1694\(97\)00041-3](https://doi.org/10.1016/S0022-1694(97)00041-3)

487 Ma Y, Zhang Y, Yang D, Farhan SB (2015) Precipitation bias variability versus various gauges  
488 under different climatic conditions over the Third Pole Environment (TPE) region. *Int J Climatol*  
489 35:1201-1211. <https://doi.org/10.1002/joc.4045>

490 Martinez WL, Martinez AR (2005) *Exploratory Data Analysis with MATLAB*. Computer  
491 Science and Data Analysis Series. Chapman and Hall/CRC Press LLC, UK.

492 Masih I, Uhlenbrook S, Maskey S, Ahmad MD (2010) Regionalization of a conceptual rainfall–  
493 runoff model based on similarity of the flow duration curve: A case study from the semi-arid  
494 Karkheh basin, Iran. *J hydrol* 391:188-201. <https://doi.org/10.1016/j.jhydrol.2010.07.018>

495 Ménégoz M, Gallée H, Jacobi HW (2013) Precipitation and snow cover in the Himalaya: from  
496 reanalysis to regional climate simulations. *Hydrol Earth Syst Sci* 17:3921–3936.  
497 <https://doi.org/10.5194/hess-17-3921-2013>  
498

499 Ndehedehe CE (2019a) The water resources of tropical West Africa: problems, progress and  
500 prospect. *Acta Geophysica* 67:621–649. <https://doi.org/10.1007/s11600-019-00260-y>  
501

502 Ndehedehe CE, Agutu NO, Okwuashi O (2018) Is terrestrial water storage a useful indicator in  
503 assessing the impacts of climate variability on crop yield in semi-arid ecosystems? *Ecol Indic* 88:  
504 51-62. <https://doi.org/10.1016/j.ecolind.2018.01.026>  
505

506 Ndehedehe CE, Anyah RO, Alsdorf D, Agutu NO, Ferreira VG (2019c) Modelling the impacts of  
507 global multi-scale climatic drivers on hydro-climatic extremes (1901–2014) over the Congo  
508 basin. *Sci Total Environ* 651:1569-1587. <https://doi.org/10.1016/j.scitotenv.2018.09.203>  
509

510 Ndehedehe CE, Ferreira VG, Agutu NO (2019b) Hydrological controls on surface vegetation  
511 dynamics over West and Central Africa. *Ecol Indic* 103:494-508.  
512 <https://doi.org/10.1016/j.ecolind.2019.04.032>  
513

514 Ndehedehe, CE, Ferreira VG, Onojeghuo AO, Agutu NO, Emengini E, Getirana A (2020a)  
515 Influence of global climate on freshwater changes in Africa's largest endorheic basin using multi-  
516 scaled indicators. *Sci Total Environ* 139643. <https://doi.org/10.1016/j.scitotenv.2020.139643>  
517

518 Ndehedehe CE, Stewart-Koster B, Burford MA, Bunn SE (2020b) Predicting hot spots of aquatic  
519 plant biomass in a large floodplain river catchment in the Australian wet-dry tropics. *Ecol*  
520 *Indic* 117:106616. <https://doi.org/10.1016/j.ecolind.2020.106616>

521 Pakoksung K, Takagi M (2016) Effect of satellite based rainfall products on river basin responses  
522 of runoff simulation on flood event. *Model Earth Syst Environ* 2:1-14.  
523 <https://doi.org/10.1007/s40808-016-0200-0>  
524

525 Prein AF, Gobiet A (2017) Impacts of uncertainties in European gridded precipitation  
526 observations on regional climate analysis. *Int J Climatol* 37:305-327.  
527 <https://doi.org/10.1002/joc.4706>

528 Price K, Purucker ST, Kraemer SR, Babendreier JE, Knightes CD (2014) Comparison of radar and  
529 gauge precipitation data in watershed models across varying spatial and temporal scales. *Hydrol*  
530 *Process.* 28:3505-3520. <https://doi.org/10.1002/hyp.9890>  
531

532 Schamm K, Ziese M, Becker A, Finger P, Meyer-Christoffer A, Schneider U, ... Stender P  
533 (2014) Global gridded precipitation over land: a description of the new GPCC First Guess Daily  
534 product. *Earth Syst Sci Data* 6: 49-60. <https://doi.org/10.5194/essd-6-49-2014>

535 Schmeier S, Shubber Z (2018) Anchoring water diplomacy–The legal nature of international  
536 river basin organizations. *J Hydrol* 567:114-120. <https://doi.org/10.1016/j.jhydrol.2018.09.054>

537 Schroth G, Läderach P, Martinez-Valle AI, Bunn C, Jassogne L (2016) Vulnerability to climate  
538 change of cocoa in West Africa: Patterns, opportunities and limits to adaptation. *Sci Total Environ*  
539 556:231-241. <https://doi.org/10.1016/j.scitotenv.2016.03.024>  
540

541 Seibert J, Vis MJ (2012) Teaching hydrological modeling with a user-friendly catchment-runoff-  
542 model software package. *Hydrol Earth Syst Sci* 16:3315-3325 [https://doi.org/10.5194/hess-16-](https://doi.org/10.5194/hess-16-3315-2012)  
543 3315-2012  
544

545 Skaskevych A, Lee J, Jung HC, Bolten J, David JL, Policelli FS, ... Ichoku CM (2020) Application  
546 of GRACE to the estimation of groundwater storage change in a data-poor region: A case study of  
547 Ngadda catchment in the Lake Chad Basin. *Hydrol Process* 34:941-955.  
548 <https://doi.org/10.1002/hyp.13613>  
549

550 Sorooshian S, Hsu KL, Gao X, Gupta HV, Imam B, Braithwaite D (2000) Evaluation of  
551 PERSIANN system satellite-based estimates of tropical rainfall. . *Bull Am Meteorol Soc* 81:2035-  
552 2046. [https://doi.org/10.1175/1520-0477\(2000\)081%3C2035:EOPSSSE%3E2.3.CO;2](https://doi.org/10.1175/1520-0477(2000)081%3C2035:EOPSSSE%3E2.3.CO;2)  
553

554 Stephens GL, L'Ecuyer T, Forbes R, Gettelmen A, Golaz JC, Bodas-Salcedo A, ... Haynes J  
555 (2010) Dreary state of precipitation in global models. *J Geophys Res-Atmos* 115 (D24).  
556 <https://doi.org/10.1029/2010JD014532>

557 Tockner K, Lorang MS, Stanford JA (2010) River flood plains are model ecosystems to test  
558 general hydrogeomorphic and ecological concepts. *River Res Appl* 26:76-86.  
559 <https://doi.org/10.1002/rra.1328>  
560

561 Vis M, Knight R, Pool S, Wolfe W, Seibert J (2015) Model calibration criteria for estimating  
562 ecological flow characteristics. *Water* 7:2358-2381. <https://doi.org/10.3390/w7052358>

563 Vu MT, Raghavan SV, Liong SY (2012) SWAT use of gridded observations for simulating  
564 runoff--a Vietnam river basin study. *Hydrol Earth Syst Sci Discuss* 16: 2801–2811.  
565 <https://doi.org/10.5194/hess-16-2801-2012>

566 Wilks D (2011) *Statistical methods in the atmospheric sciences*. Academic press, (3rd. Edition).  
567 USA.

568 Xie P, Chen M, Shi W (2010) CPC global unified gauge-based analysis of daily precipitation.  
569 In 24th Conf. on Hydrology. Atlanta, GA: American Meteorological Society.

570 Yatagai A, Kamiguchi K, Arakawa O, Hamada A, Yasutomi N, Kitoh A (2012) APHRODITE:  
571 Constructing a long-term daily gridded precipitation dataset for Asia based on a dense network  
572 of rain gauges. *Bull Am Meteorol Soc* 93:1401-1415. doi:10.1175/BAMS-D-11-00122.1

573 Zandler H, Haag I, Samimi C (2109) Evaluation needs and temporal performance differences of  
574 gridded precipitation products in peripheral mountain regions. *Sci Rep* 9:15118.  
575 <https://doi.org/10.1038/s41598-019-51666-z>

576

577

578

579

580

581  
582  
583  
584  
585  
586  
587  
588  
589  
590  
591  
592  
593  
594  
595  
596  
597  
598  
599  
600  
  
601  
  
602  
  
603  
  
604